




# Neuroprotection of Exendin-4 by Enhanced Autophagy in a Parkinsonian Rat Model of $\alpha$ -Synucleinopathy

Lu-Lu Bu<sup>1</sup> · Yi-Qi Liu<sup>1</sup> · Yan Shen<sup>1</sup> · Yun Fan<sup>1</sup> · Wen-Bo Yu<sup>1</sup> · Dong-Lang Jiang<sup>2</sup> · Yi-Lin Tang<sup>1</sup> · Yu-Jie Yang<sup>1</sup> · Ping Wu<sup>2</sup> · Chuan-Tao Zuo<sup>2</sup> · James B. Koprich<sup>1,3</sup> · Feng-Tao Liu<sup>1</sup> · Jian-Jun Wu<sup>1</sup> · Jian Wang<sup>1</sup> 

Accepted: 26 January 2021 / Published online: 15 March 2021  
© The American Society for Experimental NeuroTherapeutics, Inc. 2021

## Abstract

Glucagon-like peptide-1 (GLP-1) receptor stimulation ameliorates parkinsonian motor and non-motor deficits in both experimental animals and patients; however, the disease-modifying mechanisms of GLP-1 receptor activation have remained unknown. The present study investigated whether exendin-4 (a GLP-1 analogue) can rescue motor deficits and exert disease-modifying effects in a parkinsonian rat model of  $\alpha$ -synucleinopathy. This model was established by unilaterally injecting AAV-9-A53T- $\alpha$ -synuclein into the right substantia nigra pars compacta, followed by 4 or 8 weeks of twice-daily intraperitoneal injections of exendin-4 (5  $\mu$ g/kg/day) starting at 2 weeks after AAV-9-A53T- $\alpha$ -synuclein injections. Positron emission tomography/computed tomography (PET/CT) scanning and immunostaining established that treatment with exendin-4 attenuated tyrosine-hydroxylase-positive neuronal loss and terminal denervation and mitigated the decrease in expression of vesicular monoamine transporter 2 within the nigrostriatal dopaminergic systems of rats injected with AAV-9-A53T- $\alpha$ -synuclein. It also mitigated the parkinsonian motor deficits assessed in behavioral tests. Furthermore, through both in vivo and in vitro models of Parkinson's disease, we showed that exendin-4 promoted autophagy and mediated degradation of pathological  $\alpha$ -synuclein, the effects of which were counteracted by 3-methyladenine or chloroquine, the autophagic inhibitors. Additionally, exendin-4 attenuated dysregulation of the PI3K/Akt/mTOR pathway in rats injected with AAV-9-A53T- $\alpha$ -synuclein. Taken together, our results demonstrate that exendin-4 treatment relieved behavioral deficits, dopaminergic degeneration, and pathological  $\alpha$ -synuclein aggregation in a parkinsonian rat model of  $\alpha$ -synucleinopathy and that these effects were mediated by enhanced autophagy via inhibiting the PI3K/Akt/mTOR pathway. In light of the safety and tolerance of exendin-4 administration, our results suggest that exendin-4 may represent a promising disease-modifying treatment for Parkinson's disease.

**Keywords** Exendin-4 · Parkinson's disease · Neuroprotection ·  $\alpha$ -synuclein · Autophagy · Vesicular monoamine transporter 2 neuroimaging

Lu-Lu Bu, Yi-Qi Liu, and Yan Shen contributed equally to this work.

## Highlight

- We found that exendin-4 significantly ameliorated motor deficits and attenuated nigral tyrosine-hydroxylase-positive neuronal loss and striatal dopaminergic denervation in an AAV9-induced parkinsonian rat model of  $\alpha$ -synucleinopathy, all of which recapitulated features of the natural progression of Parkinson's disease.
- VMAT-2 PET/CT scanning demonstrated that exendin-4 mitigated synaptic dysfunction in parkinsonian rats.
- Exendin-4 increased the formation of autophagosomes and resulted in the clearance of pathological  $\alpha$ -synuclein via enhanced autophagy, which may be mediated by inhibition of the PI3K/Akt/mTOR pathway.

Extended author information available on the last page of the article

## Introduction

Parkinson's disease (PD) is a slowly progressive neurodegenerative disorder that is characterized by parkinsonian motor deficits and numerous non-motor symptoms [1]. The crucial pathological features of PD are loss of dopaminergic neurons within the substantia nigra pars compacta (SNpc), the presence of Lewy bodies, and neuroinflammation [2]. Although there are available therapies to treat symptoms of PD, there is currently no disease-modifying treatment that slows or halts the neurodegenerative process of PD [3].

Growing evidence has demonstrated that patients with Type-2 diabetes (T2DM) have an increased risk of developing PD, and their similar dysregulation in terms of underlying pathological mechanisms suggests that treatments for T2DM may represent potential strategies for treating PD

[4]. Exenatide, a glucagon-like peptide-1 (GLP-1) receptor agonist, which is a synthetic form of naturally occurring reptilian hormone of exendin-4 (Ex-4) [5], is approved for the treatment of T2DM and exhibits neuroprotective effects in many preclinical animal models and cell lines of various neurological disorders, such as stroke [6], traumatic brain injury [7], Alzheimer's disease (AD) [8], amyotrophic lateral sclerosis (ALS) [9], and PD [6, 10]. Many previous studies have also shown that GLP-1 receptors (GLP-1Rs) are widely expressed in many regions throughout the central nervous system, especially in the SNpc and striatum in both humans and animal models [11]. Ex-4 has been demonstrated to cross the blood-brain barrier to attenuate nigral dopaminergic neuronal loss and striatal dopaminergic-fiber denervation, as well as to reduce neuroinflammation and alleviate motor deficits in an increasing array of parkinsonian animal models [12]. A proof-of-concept study [13, 14] and a randomized, placebo-controlled trial [15] of exenatide have also exhibited positive effects on mitigating motor deficits in PD patients; however, the disease-modifying effects still need to be examined further. Despite the pivotal role of accumulating  $\alpha$ -synuclein ( $\alpha$ -syn) in the pathogenesis of PD, previous studies regarding the neuroprotective effects of Ex-4 have mainly focused on classical neurotoxin-based PD models. Therefore, whether Ex-4 treatment can produce similar results in an accumulating  $\alpha$ -synucleinopathy-based parkinsonian model remains unclear.

In light of the excellent safety profile of Ex-4 in T2DM patients, as well as the encouraging results of preclinical studies demonstrating its neuroprotective properties, Ex-4 represents an attractive therapeutic option for PD. In the present study, we utilized a parkinsonian rat model of  $\alpha$ -synucleinopathy, established by unilateral injection of an  $\alpha$ -syn-overexpression adeno-associated virus serotype 9 (AAV-9) construct, to recapitulate the progressive accumulation of pathogenic  $\alpha$ -syn in the nigrostriatal system that is observed in sporadic PD patients [16]. The neuroprotective effects of Ex-4 were assessed via an array of measurements at different time points. Our findings suggest that Ex-4 may be useful as a disease-modifying regimen to mitigate the neurodegenerative process of PD.

## Materials and Methods

### Ethics Statement

All animal studies were approved by the Ethics Committee in the Department of Laboratory Animal Science at Fudan University (Shanghai, China). The approval number is 20171552A498. All efforts were done to reduce animal suffering during the experimental period.

### Animals and Stereotaxic Injections

The plasmids (pAAV-CAG-MCS) for the production of AAV-9 inducing the overexpression of hA53T- $\alpha$ -syn with a 3xFlag tag, driven by the chicken beta actin (CBA/CAG) promoter, were produced by Biowit (Shenzhen, China). The control vector was constructed by omitting the hA53T- $\alpha$ -syn sequence. The concentration of pAAV-CAG-3xFlag-hA53T- $\alpha$ -syn virus (AAV-A53T- $\alpha$ -syn) was  $5.08353 \times 10^{12}$  vg/ml, and the titer of the AAV9 vehicle virus (AAV-vehicle) was  $5.5525 \times 10^{12}$  vg/ml. We observed that female rats were less aggressive and weighed less than male rats, so, for convenience given the daily nature of our processes and the large number of rats, we performed all experiments on female rats. Three-month-old female Sprague-Dawley rats (Department of Laboratory Animal Science, Fudan University, Shanghai, China), weighing approximately 250–280 g, were used for stereotaxic injections. Surgery was performed as described previously [17]. Briefly, rats were anesthetized and placed in a stereotaxic head frame (RWD, Shenzhen, China). An injection needle (33 gauge) on a 5- $\mu$ L Hamilton syringe was stereotaxically inserted into the SNpc region of the right hemisphere (anteroposterior,  $-5.2$  mm; mediolateral,  $-2.0$  mm; dorsoventral,  $-7.5$  mm, from skull at bregma, according to the atlas of Paxinos and Watson [18]). A total of 2  $\mu$ L of the viral solution of AAV-vehicle or AAV-A53T- $\alpha$ -syn was injected at a rate of 0.2  $\mu$ L/min. The numbers of experimental rats used for each experiment are listed in Additional file 1: Table S1.

### Ex-4 Treatment

The experimental design for Ex-4 treatments is shown in Fig. 1a. At 2-week post-injection (2 w.p.i.), all rats were randomized (according to a random number table produced with a computer) to treatment with either Ex-4 (E7144, Sigma-Aldrich) or normal saline (NS). All rats received twice-daily intraperitoneal injections of Ex-4 (1.25  $\mu$ g/mL dissolved in normal saline, 5  $\mu$ g/kg/day) or normal saline according to their body weight, which was measured every week (Additional file 1, Figure S1), until they were sacrificed.

### Behavioral Analysis

Behavioral tests (Rotarod test and Cylinder test) were performed before surgeries to ensure intact motor functions at baseline and were performed again at 2, 6, and 10 w.p.i. to evaluate parkinsonian behavioral deficits.

**Rotarod Test.** According to a previous method [19], rats were placed on a rotarod accelerating slowly from 4 to

40 rpm within 5 min, and the duration that each rat remained on the rotarod was measured. The rats were trained once, 3 days before the test, and each rat was assessed three times with at least a 1-h interval between trials. The final data are presented as the mean duration of three consecutive trials.

**Cylinder Test.** Spontaneous movement was measured by placing rats in a transparent cylinder (height, 30 cm; diameter, 20.4 cm). Spontaneous activity of forelimbs was recorded for 6 min, and the number of forepaw touches of each side was counted. We excluded rats who did not perform at least 20 forepaw touches. According to our previous work [17], the final data are presented as the percent of asymmetry between use of the left (contralateral to the injection) and right paw (ipsilateral to the lesion), calculated by the following equation:  $((\% \text{ right paw use}) - (\% \text{ left paw use})) / ((\% \text{ right paw use}) + (\% \text{ left paw use})) * 100$ .

## Micro PET/CT Imaging

To evaluate dopaminergic synaptic disruption in the striatum *in vivo*, PET/CT scanning of vesicular monoamine transporter 2 (VMAT-2) was conducted at weeks two, six, and ten after the surgeries. Each rat was injected intravenously (via the caudal vein) with approximately 37 MBq (1 mCi)

of  $^{18}\text{F}$ -Fluoropropyl-(+)-dihydrotrabenazine ( $^{18}\text{F}$ -FP-(+)-DTBZ) and was then scanned after a 1-h uptake period. Randomly selected rats in the AAV-vehicle and AAV-A53T- $\alpha$ -syn groups were alternately scanned under continual 3% isoflurane anesthetization using an Inveon PET/CT scanner (SIEMENS, Germany). The PET and anatomic CT images were reconstructed via the manufacturer's software. The regions of interest (ROIs) were delineated and further analyzed via PMOD software (Ver. 3.2, PMOD Technologies, Zurich, Switzerland). The standardized uptake values (SUVs) of the left striatum, right striatum, and cerebellum were quantitatively determined with the following computational formula:  $\text{SUV} = \text{measured radioactivity concentration in ROIs} / (\text{injection dose} / \text{body weight})$ . With the cerebellum serving as the internal control, the SUV ratio (SUVR) of the left and right striatum was determined as follows:  $\text{SUVR} = (\text{SUV}_{\text{striatum}} - \text{SUV}_{\text{cerebellum}}) / \text{SUV}_{\text{cerebellum}}$ .

## Immunofluorescence

Rats were sacrificed by intraperitoneal injection of 2% sodium pentobarbital, followed by perfusion with ice-cold PBS and 4% paraformaldehyde. The brains were removed, post-fixed overnight in 4% paraformaldehyde, and then

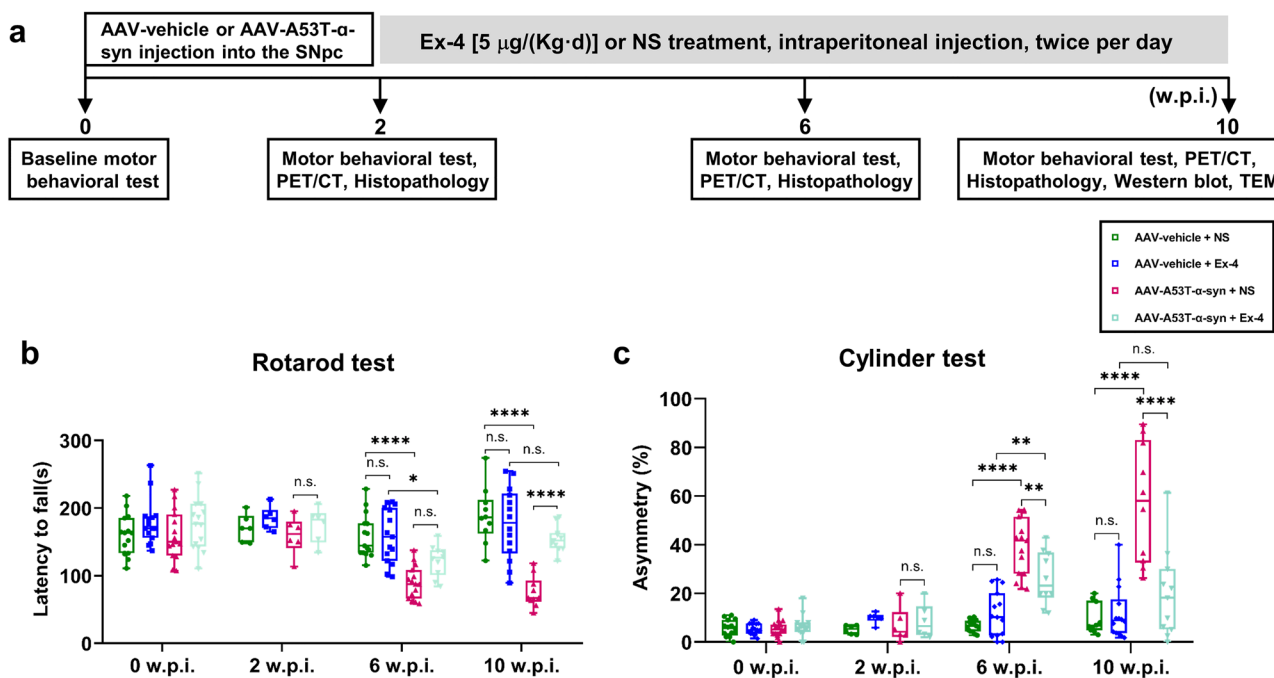
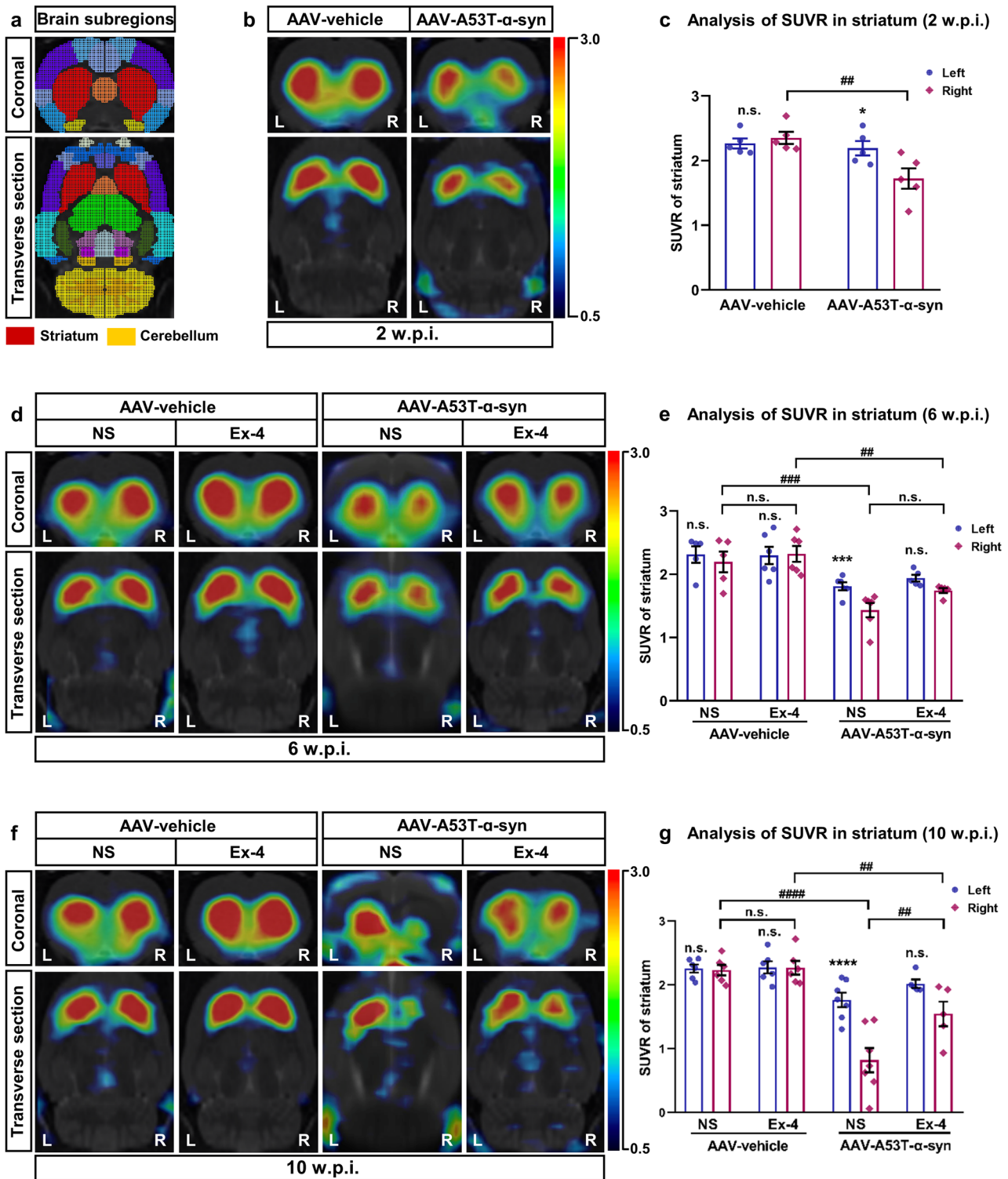


**Fig. 1** Ex-4 treatment attenuates parkinsonian motor deficits in AAV-A53T- $\alpha$ -syn-injected rats. **(a)** Schematic work-flow of this study. Behavioral assessments of motor coordination **(b)**, rotarod test) and forepaw usage asymmetry **(c)**, cylinder test) in AAV-vehicle + NS/Ex-4 and AAV-A53T- $\alpha$ -syn + NS/Ex-4 group rats at 0 w.p.i. ( $n = 15$  biologically independent animals), 2 w.p.i. ( $n = 6$ ), 6 w.p.i. ( $n = 15$ , 15, 10) and 10 w.p.i. ( $n = 10$ , 14, 10, 11). Exendin-4 treatment

restored the parkinsonian motor deficits induced by unilateral AAV-A53T- $\alpha$ -syn injection at 10 w.p.i. Data are presented as median with min to max. Statistical significance was determined using an ordinary Two-way ANOVA followed by Tukey's post hoc tests. \* $p < 0.05$ , \*\* $p < 0.01$ , \*\*\*\* $p < 0.0001$ ; n.s., not significant. Ex-4 exendin-4, NS normal saline, w.p.i. weeks post injection



cryoprotected in consecutive incubations in 20% and 30% sucrose solutions (w/v in 0.1 M PBS) before being embedded in OCT and sectioned via a cryostat (Leica). Immunofluorescence was performed on free-floating 30- $\mu$ m-thick serial brain sections. The brain slices were permeabilized

with 0.3% Triton X-100 in PBS and were incubated with primary antibodies against pSer129- $\alpha$ -syn (1:200, ab51253, Abcam) and tyrosine hydroxylase (TH, 1:1000, MAB318, Merck) overnight at 4 °C. Then, the sections were incubated with 0.3% Triton X-100/PBS and a mixture of secondary



**Fig. 2**  $^{18}\text{F}$ -FP-(+)-DTBZ PET/CT scanning of the striatal standardized uptake value ratios (SUVRs) in AAV-vehicle-injected and AAV-A53T- $\alpha$ -syn-injected rats. **(a)** Schematic coronal and transverse plane view of rat striatum (indicated by red areas). **(b)** Representative PET/CT images of the coronal and transverse striatum planes of a AAV-vehicle-injected (left column) and a AAV-A53T- $\alpha$ -syn-injected rat (right column) at 2 w.p.i. **(c)** Statistical analysis and comparison of the striatal SUVR in AAV-vehicle-injected ( $n = 5$ ) and AAV-A53T- $\alpha$ -syn-injected ( $n = 5$ ) rats. **(d, f)** Representative striatal PET/CT images of the AAV-vehicle-injected (left panel) and AAV-A53T- $\alpha$ -syn-injected rats (right panel) treated with NS (normal saline) or Ex-4 (exendin-4) at 6 w.p.i. **(d)** and 10 w.p.i. **(f)**. **(e, g)** Statistical analysis and comparison of the striatal SUVR in AAV-vehicle-injected and AAV-A53T- $\alpha$ -syn-injected rats at 6 w.p.i. **(e)**, ( $n = 5, 6, 6, 5$ ) and 10 w.p.i. **(g)**, ( $n = 6, 6, 7, 5$ ). Data are presented as mean  $\pm$  SEM. Statistical significance was determined using a repeated-measures Two-way ANOVA followed by Tukey's post hoc tests, or paired/unpaired Student's  $t$  test at 2 w.p.i. \* $p < 0.05$ , \*\*\* $p < 0.001$ , \*\*\*\* $p < 0.0001$ , Left versus Right; ## $p < 0.01$ , ### $p < 0.001$ , #### $p < 0.0001$ . n.s., not significant, w.p.i. weeks post injection

antibodies (1:1000, goat-anti-rabbit Alexa Fluor 488 and goat-anti-mouse Alexa Fluor 555, Invitrogen) at room temperature (RT) for 2 h. After sections were washed with PBS, sections were coverslipped and mounted with DAPI-mounting solution. The fluorescent images were acquired via an Olympus VS120 Virtual Microscopy Slide Scanning System.

### Immunohistochemistry and Quantitative Analysis

For immunohistochemical staining, free-floating 30- $\mu\text{m}$  sections were quenched for endogenous peroxidases in a 3% hydrogen peroxide solution. Then, the sections were blocked with 5% BSA/PBS, 5% goat serum plus 0.3% Triton X-100, and were then incubated with a primary antibody against TH (1:2000, ab112, Abcam) at 4 °C overnight, followed by incubation with a biotin-conjugated goat-anti-rabbit secondary antibody (1:3000, BA-1000, Vector Laboratories, Burlingame, CA) for 2 h at RT and subsequent incubation in avidin-biotin complex (1:1000, PK-6100, Vector) for 3 h at RT. After incubation with a DAB-peroxidase substrate (SK-4100, Vector), sections were counterstained with Nissl (C0117, Beyotime, Shanghai, China).

The TH-positive neurons from the right SNpc region were counted through optical fractionators, and the unbiased method for cell counting consisted of a photomicroscope (Olympus) and Stereo Investigator software (MBF Biosciences, Williston, VT). The fiber density in the striatum was analyzed by measuring the optical density (OD) via ImageJ software (NIH, USA). For each rat, three representative striatal sections were analyzed (at bregma 2.16, 0.72, and -1.20 mm, according to the atlas of Paxinos and Watson (6th edition, 2007)). The OD value of each section was calculated as the OD value of the right striatum minus that of the background, and the mean of three sections represented

the final striatal OD value of each rat. The relative TH fiber density was standardized with that of the AAV-vehicle (+NS) group.

### Transmission Electron Microscopy

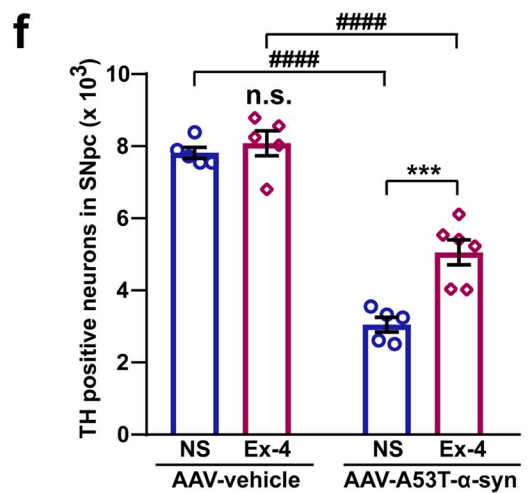
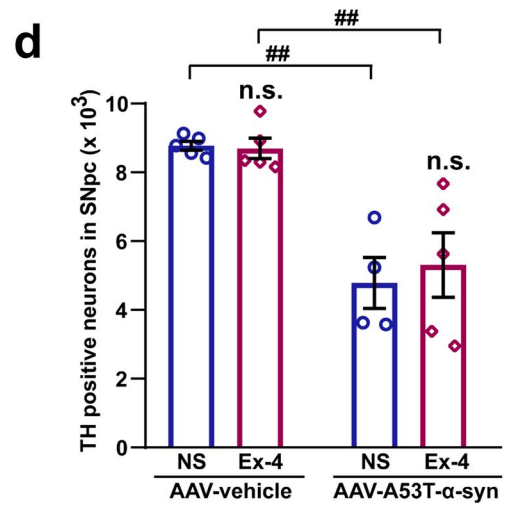
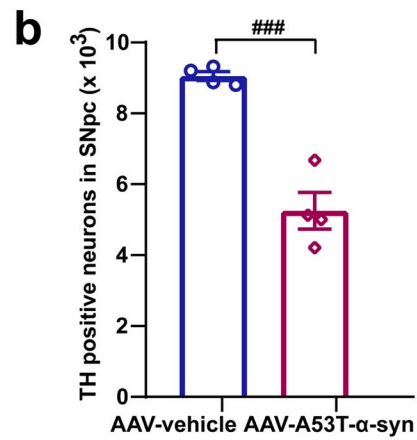
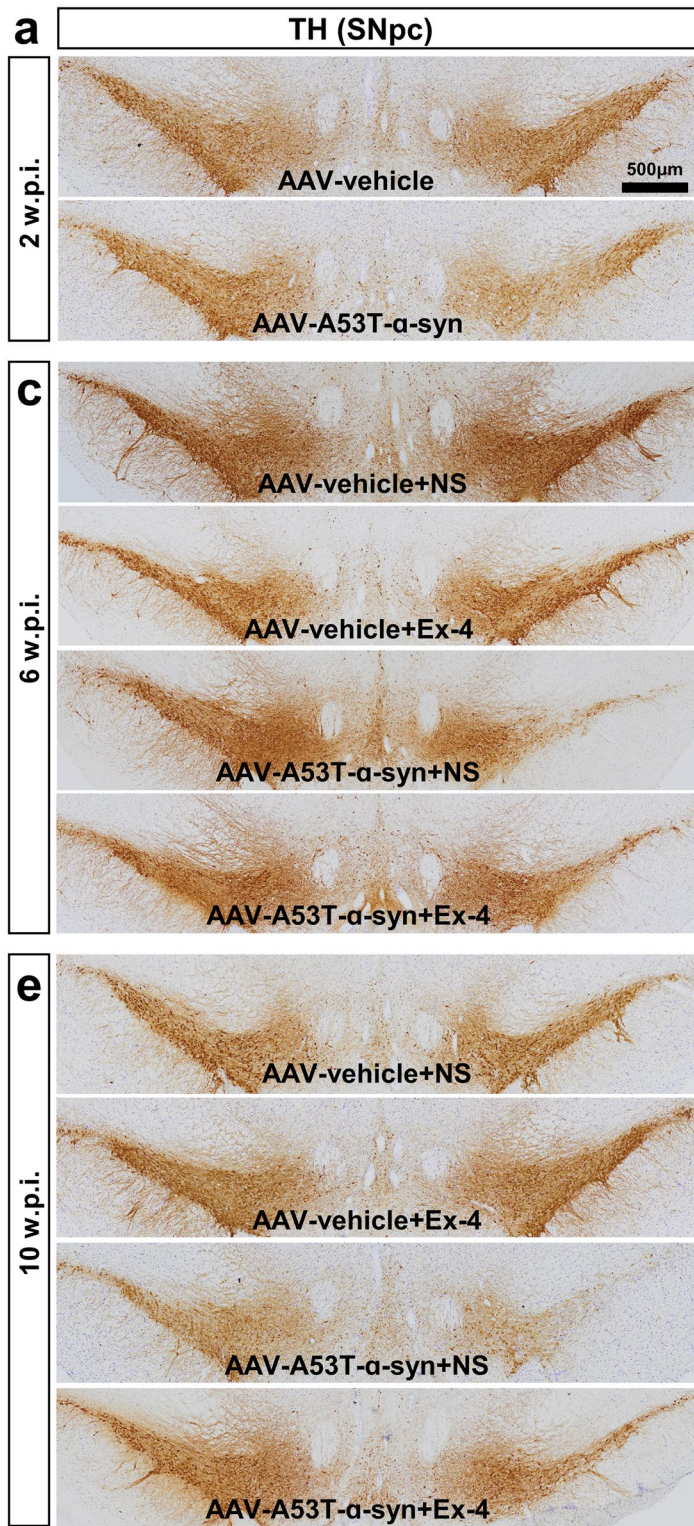
The rats used for transmission electron microscopy (TEM) were randomly selected from each group at 10 w.p.i. ( $n = 3$ ). After perfusion with ice-cold PBS and 4% paraformaldehyde plus 1% glutaraldehyde (in 0.1 M PBS), the harvested brain tissue was sectioned via a vibratome, and a total of 2 mm<sup>3</sup> of tissue from the middle part of the SNpc in the right hemisphere was used. This tissue was post-fixed in 2.5% glutaraldehyde/PBS overnight at 4 °C, after which it was incubated for 1 h in 1% osmium tetroxide/PBS, dehydrated using graded alcohols, and embedded in polybed 812 resin. After polymerization at 60 °C for 48 h, 80-nm ultrathin sections were prepared with a Leica Ultracut UCT slicer (Leica EM UC6, Germany). After being stained with uranyl acetate and lead citrate, the sections were observed under TEM (PHILIPS CM-1200) for the assessment of autophagosomes in SNpc dopaminergic neurons.

### Cell Culture and Drug Interventions

SH-SY5Y cells stably overexpressing hA53T- $\alpha$ -syn were constructed by Dr. Feng-tao Liu and have been reported in our previous study [20]. SH-SY5Y cells were pretreated with 5 mM of 3-methyladenine (3-MA, M9281, Sigma) or 50  $\mu\text{M}$  chloroquine (C6628, Sigma) for 10 min to inhibit autophagy, and 100 nM of Ex-4 was added for 48 h for the following experiments. In addition, to further exclude the influence of continuous  $\alpha$ -syn overexpression, cycloheximide (CHX, 10  $\mu\text{M}$ , Sigma) was given to inhibit protein synthesis for 60 min before Ex-4 treatment. Subsequently, cells were prepared for Western blotting and immunocytochemistry.

### Immunoblotting Analysis

Total tissues or cell lysates were prepared by homogenization in RIPA buffer (Thermo Fisher Scientific) containing a mixture of proteinase and phosphatase inhibitors (Thermo Fisher Scientific). Whole protein content was quantified using a BCA Kit (Thermo Fisher Scientific). A total of 30  $\mu\text{g}$  of protein was electrophoresed on 4–20% SDS-PAGE gels and was then transferred onto PVDF membranes. The membranes were blocked using blocking solution (Tris-buffered saline with 5% non-fat dry milk and 0.1% Tween-20) for 1 h and were then incubated at 4 °C overnight with the following primary antibodies (all dilutions, 1:1000): anti-TH (ab112), anti- $\alpha$ -syn (ab138501), anti-pSer129- $\alpha$ -syn (ab51253), anti-LAMP1 (ab24170), anti-SQSTM1/p62 (ab109012),



and anti-LC3B (ab192890) from Abcam; anti-PI3K-p85(CST4257), anti-phospho-mTOR (Ser2448) (CST5536), anti-phospho-AKT (Thr308) (CST13038), and anti-beclin-1 (CST3495) from Cell Signaling Technology, and anti-GAPDH from Yishan Biotechnology.

The membranes used for  $\alpha$ -syn and pSer129- $\alpha$ -syn detection were incubated with 4% paraformaldehyde plus 0.1% glutaraldehyde (in 0.1 M PBS) for 30 min at RT



**Fig. 3** Ex-4 treatment mitigates TH-positive neuronal degeneration in AAV-A53T- $\alpha$ -syn-injected rats. Representative TH immunostaining photomicrographs from coronal mesencephalon sections containing TH-positive neurons in the SNpc region of AAV-vehicle-injected and AAV-A53T- $\alpha$ -syn-injected rats at 2 (a), 6 (c), and 10 w.p.i. (e) time-points. Unbiased stereological counts of TH-positive neurons in the right SNpc region in AAV-vehicle-injected and AAV-A53T- $\alpha$ -syn-injected rats at 2 (b), 6 (d), and 10 w.p.i. (f). AAV-A53T- $\alpha$ -syn injection induced death of TH-positive neurons in the right SNpc region, which was halted by Ex-4 treatment. Error bars represent the mean  $\pm$  SEM. Statistical significance was determined using a two-way ANOVA followed by Tukey's post hoc tests.  $^{##}p < 0.01$ ,  $^{###}p < 0.001$ ,  $^{####}p < 0.0001$ , AAV-A53T- $\alpha$ -syn-injected rats versus AAV-vehicle-injected rats;  $^{***}p < 0.001$ , Ex-4 treatment group versus NS treatment group; n.s., not significant, NS treatment group versus Ex-4 treatment group. Sample size: AAV-vehicle-injected and AAV-A53T- $\alpha$ -syn-injected rats at 2 w.p.i. ( $n = 4, 4$ ); AAV-vehicle + NS/Ex-4 and AAV-A53T- $\alpha$ -syn + NS/Ex-4 group rats at 6 w.p.i. ( $n = 5, 5, 4, 5$ ) and 10 w.p.i. ( $n = 5, 5, 5, 6$ ), respectively. Please note that the statistical analysis in (b) was determined by a two-tailed unpaired Student's  $t$  test. Ex-4/exendin-4, NS normal saline, w.p.i. weeks post injection. Scale bars = 500  $\mu$ m for (a),(c), and (e)

before blocking for improved detection [21]. Then, the membranes were incubated with HRP-conjugated secondary antibody (1: 20,000, Jackson ImmunoResearch, PA, USA) for 2 h at RT. All antibodies were diluted in blocking solution. The membranes were visualized using an enhanced chemiluminescence system (Thermo Fisher Scientific) and were analyzed with ImageJ software.

### Immunocytochemistry

SH-SY5Y cells were fixed with methanol for 10 min at 4 °C, followed by permeabilization with 0.3% Triton X-100 in PBS and incubation with primary antibodies against LC3B (1:1000, ab192890, Abcam) and LAMP1 (1:1000, sc-20011, Santa Cruz Biotechnology) overnight at 4 °C. Then the cells were incubated with 0.3% Triton X-100/PBS and a mixture of secondary antibodies (1:1000, goat-anti rabbit Alexa Fluor 594 and goat-anti-mouse Alexa Fluor 488, Invitrogen) at RT for 2 h. After washing with PBS for three times, cells were mounted with DAPI-mounting solution, and z-stack images were captured on a laser scanning confocal microscope (FV-1000, Olympus).

### Statistical Analysis

Statistical analysis was carried out using GraphPad Prism 7 software. All data, except the results of behavioral analysis, are presented as the mean  $\pm$  standard error of the mean (SEM) from at least three independent experiments. Representative images were selected from at least three experiments with similar results. Statistical significance for multi-factor analysis was determined using ordinary or repeated-measures two-way analysis of variance (ANOVA) followed by Tukey's post hoc tests for pairwise comparisons.

Single-factor analysis was determined via one-way ANOVAs or paired/unpaired Student's  $t$  tests.  $P < 0.05$  was considered to be statistically significant.

## Results

### Ex-4 Treatment Rescues Parkinsonian Motor Deficits in Rats Receiving AAV-A53T- $\alpha$ -syn Injections

A core feature of PD is predominant motor deficit. Hence, we assessed motor coordination and autonomous forepaw touches via rotarod and cylinder tests, respectively, at each time point. Compared with that of AAV-vehicle-injected rats, unilateral AAV-A53T- $\alpha$ -syn injections elicited progressive deterioration of motor function and resulted in significant asymmetry and decreased latency to fall at 6 w.p.i. and 10 w.p.i. (all  $p < 0.0001$ ; Fig. 1b, c). Ex-4 treatments in AAV-A53T- $\alpha$ -syn-injected rats significantly reduced asymmetric forepaw touches, as measured by the cylinder test at 6 w.p.i. ( $p = 0.0092$ ), and led to comparable results to those of AAV-vehicle-injected rats treated with/without Ex-4 in both behavioral assessments at 10 w.p.i. ( $p < 0.0001$ ).

### Ex-4 Treatment Alleviates Striatal Dopaminergic Dysfunction Measured by $^{18}$ F-DTBZ VMAT-2 PET Imaging In Vivo

In order to assess the effect of Ex-4 on the uptake ability of striatal dopaminergic VMAT-2 in AAV-A53T- $\alpha$ -syn-injected rats, we utilized  $^{18}$ F-FP-(+)-DTBZ PET/CT scanning to assess the synaptic function of the nigrostriatal system. At 2 w.p.i., there was a significant decrease in the SUVR of the right striatum in the AAV-A53T- $\alpha$ -syn group compared with that in AAV-vehicle counterparts ( $-26.74\%$ ,  $p = 0.0089$ ; Fig. 2b, c). Following treatment with NS since 2 w.p.i., AAV-A53T- $\alpha$ -syn-injected rats displayed a continuous reduction of the right striatal SUVR from 2 to 10 w.p.i., which was significantly different from that in AAV-vehicle-injected rats treated with NS ( $-34.69\%$ ,  $p = 0.002$  at 6 w.p.i. and  $-63.28\%$ ,  $p < 0.0001$  at 10 w.p.i.; Fig. 2d–g). In contrast, after the administration of Ex-4 for 4 or 8 weeks, the reduction in the right-sided striatal SUVR in AAV-A53T- $\alpha$ -syn-injected rats was nearly stopped ( $-24.98\%$  at 6 w.p.i. and  $-31.88\%$  at 10 w.p.i., vs AAV-vehicle + Ex-4 group), which was significantly different at 10 w.p.i. ( $p = 0.0014$ ) compared with that of AAV-A53T- $\alpha$ -syn-injected rats treated with NS. Additionally, the difference in the SUVR between the left and right striatum was also decreased via Ex-4 treatment. In addition, despite the unilateral injection of AAV-A53T- $\alpha$ -syn into

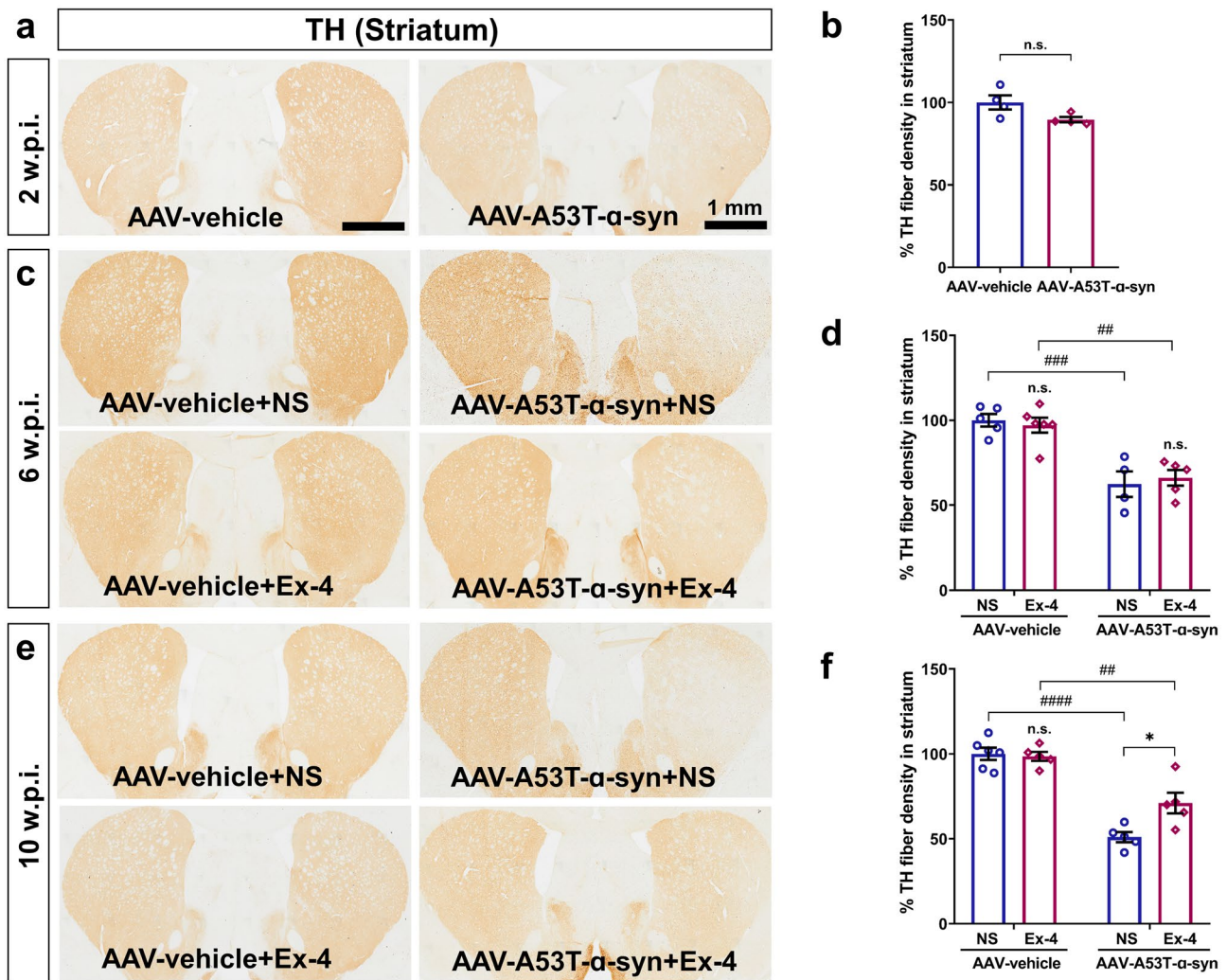


**Fig. 4** Ex-4 treatment ameliorates striatal dopaminergic terminal denervation in AAV-A53T- $\alpha$ -syn-injected rats. Representative striatal TH immunostaining in the AAV-vehicle-injected and AAV-A53T- $\alpha$ -syn-injected rats at 2 (**a**), 6 (**c**), and 10 w.p.i. (**e**) time-points. Statistical analysis and comparison of the striatal optical density of the TH immunostaining in AAV-vehicle-injected and AAV-A53T- $\alpha$ -syn-injected rats at 2 (**b**), 6 (**d**), and 10 w.p.i. (**f**). The AAV-A53T- $\alpha$ -syn injection induced striatal dopaminergic terminal denervation, which was stopped by Ex-4 treatment. Error bars represent the mean  $\pm$  SEM. Statistical significance was determined using a two-way

ANOVA followed by Tukey's post hoc tests.  $^{##}p < 0.01$ ,  $^{###}p < 0.001$ ,  $^{####}p < 0.0001$ , AAV-vehicle-injected rats versus AAV-A53T- $\alpha$ -syn-injected rats;  $^{*}p < 0.05$ , Ex-4 treatment group versus NS treatment group; n.s., not significant. Sample size: AAV-vehicle and AAV-A53T- $\alpha$ -syn group rats at 2 w.p.i. ( $n = 4, 4$ ); AAV-vehicle + NS/Ex-4 and AAV-A53T- $\alpha$ -syn + NS/Ex-4 group rats at 6 w.p.i. ( $n = 5, 6, 4, 5$ ) and 10 w.p.i. ( $n = 6, 5, 5, 5$ ), respectively. Please note that the statistical analysis in (**b**) was determined by two-tailed unpaired Student's  $t$  test. Ex-4/exendin-4, NS/normal saline, w.p.i. weeks post injection. Scale bars = 1 mm for (**a**), (**c**), and (**e**)

the right SNpc, there was mild SUVR reduction in the contralateral striatum regardless of whether rats were treated with NS or Ex-4.

### Ex-4 Treatment Mitigates Nigrostriatal Dopaminergic Degeneration and Pathologic $\alpha$ -syn Aggregation

To further test the alleviation of pathological changes in this parkinsonian rat model of  $\alpha$ -synucleinopathy, we performed nigrostriatal TH and pS129- $\alpha$ -syn immunostaining at different time

points. As shown in Fig. 3 a and b, AAV-A53T- $\alpha$ -syn injection induced a significant loss of TH-positive neurons in the SNpc at 2 w.p.i. ( $-42\%$  vs AAV-vehicle group,  $p = 0.0004$ ), which became more severe at 6 w.p.i. ( $-45\%$  vs AAV-vehicle + NS group) and 10 w.p.i. ( $-61\%$ ) (Fig. 3c-f). This progressive neuronal loss was nearly stopped via long-term Ex-4 treatment ( $-39\%$  at 6 w.p.i. and  $-37\%$  at 10 w.p.i., vs AAV-vehicle + Ex-4 group) and was significantly alleviated at 10 w.p.i. compared with that of NS treatment ( $p = 0.0005$ ). Consistent with the results of TH-positive neuronal counts in the SNpc, the progressive reduction of striatal TH immunoreactivity induced by



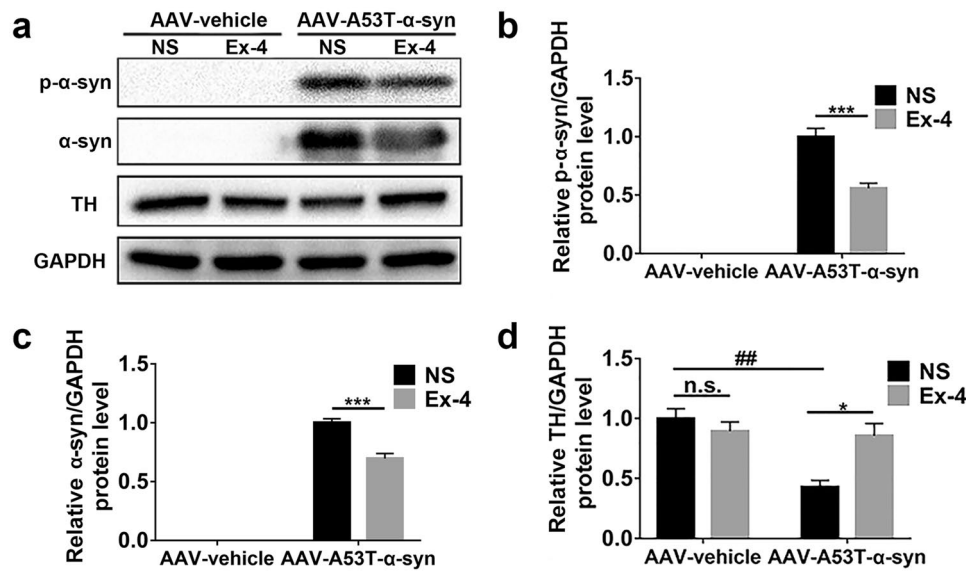


**Fig. 5** Ex-4 treatment decreases the expression of pS129- $\alpha$ -syn and total  $\alpha$ -syn and preserves the expression of TH in AAV-A53T- $\alpha$ -syn-injected rats. The total ventral midbrain (VMB) lysates of AAV-vehicle-injected or AAV-A53T- $\alpha$ -syn-injected rats were collected ( $n = 4$  biologically independent animals for each group), electrophoresed and immunoblotted. **(a)** Western blot showing the expression of pS129- $\alpha$ -syn, total  $\alpha$ -syn, and TH upon NS or Ex-4 treatment in AAV-vehicle-injected and AAV-A53T- $\alpha$ -syn-injected rats. **(b–d)** The quantitative analysis of the expression of pS129- $\alpha$ -syn, total  $\alpha$ -syn,

and TH were normalized to the GAPDH expression level. Error bars represent the mean  $\pm$  SEM of at least three independent experiments with similar results. Each sample was composed of lysates equally pooled from four rats. Statistical significance was determined using a Two-way ANOVA followed by Tukey's post hoc tests. \* $p < 0.05$ , \*\*\* $p < 0.001$ , NS-treated rats versus Ex-4-treated rats; ## $p < 0.01$ , AAV-vehicle-injected rats versus AAV-A53T- $\alpha$ -syn-injected rats; n.s. not significant, Ex-4 extendin-4, NS normal saline

AAV-A53T- $\alpha$ -syn ( $-10.42\%$  at 2 w.p.i.,  $-37.65\%$  at 6 w.p.i., and  $-49.01\%$  at 10 w.p.i., vs AAV-vehicle + NS group) was largely slowed by Ex-4 treatment ( $-31.98\%$  at 6 w.p.i. and  $-27.93\%$  at 10 w.p.i., vs AAV-vehicle + Ex-4 group) and was significantly halted at 10 w.p.i. ( $p = 0.0151$ ; Fig. 4). Western-blot analysis also revealed that the AAV-A53T- $\alpha$ -syn-mediated reduction of TH was restored by Ex-4 in the ventral midbrain at 10 w.p.i. (Fig. 5a, d).

Next, pSer129- $\alpha$ -syn/TH double immunostaining was used to monitor the progression of pathologic  $\alpha$ -syn induced by AAV-A53T- $\alpha$ -syn injection. Despite the strong expression of  $\alpha$ -syn at 2 w.p.i. (Additional file 1: Figure S2), there was only limited pSer129- $\alpha$ -syn immunoreactivity with considerable loss of TH-positive neurons in the SNpc (Fig. 6). Accompanied by progressive TH-positive neuronal death in AAV-A53T- $\alpha$ -syn-injected rats treated with NS at 6 w.p.i., more pSer129- $\alpha$ -syn was accumulated and co-localized with almost all residual TH-positive neurons in the SNpc. At 10 w.p.i., only a few TH-positive neurons survived, and a mass of pSer129- $\alpha$ -syn aggregates was observed (Additional file 1: Figure S3). Strikingly, Ex-4 treatment significantly mitigated SNpc dopaminergic neuronal loss and largely decreased pathological pSer129- $\alpha$ -syn accumulation at 6 and 10 w.p.i. Furthermore, Western-blot analysis also confirmed a substantial decrease of total  $\alpha$ -syn and pSer129- $\alpha$ -syn immunoreactivity in the ventral midbrain of AAV-A53T- $\alpha$ -syn-injected rats following Ex-4 treatment (Fig. 5a–c).

### Ex-4 Treatment Activates Autophagic Pathways

Our present findings suggested that Ex-4 treatment decreased  $\alpha$ -syn pathology induced by AAV-A53T- $\alpha$ -syn injection. In light of the pivotal role of autophagy in the clearance of pathological misfolded proteins [22], we hypothesized that activation of autophagic pathways may be involved in Ex-4-mediated degradation of pathological  $\alpha$ -syn. To test this hypothesis, we constructed SH-SY5Y cells that stably over-expressed human A53T- $\alpha$ -syn, and then added Ex-4 with or without 3-MA and chloroquine for 48 h. Immunoblotting showed that mutant  $\alpha$ -syn accumulation was significantly reduced in Ex-4 treated group, accompanied with the significantly increased level of LAMP1 and beclin-1 expression and LC3B-II/LC3B-I ratio ( $p < 0.0001$ ,  $p = 0.0154$ , and  $p = 0.0010$ , respectively), as well as the decreased level of p62 accumulation ( $p = 0.0388$ ; Fig. 7a, b). Furthermore, the immunocytochemistry also demonstrated the increased LC3B puncta that are positive for LAMP1 in Ex-4 treated SH-SY5Y cells (Fig. 7c). All these results indicated the substantial upregulation of the autophagic flux by Ex-4 treatment. Meanwhile, the autophagic inhibitors, 3-MA and chloroquine, completely reversed the activation of autophagic pathway, and eliminated the protective effect of Ex-4 in  $\alpha$ -syn clearance (Fig. 7a–c). In addition, to observe the accurate clearance of existing  $\alpha$ -syn in SH-SY5Y cells,

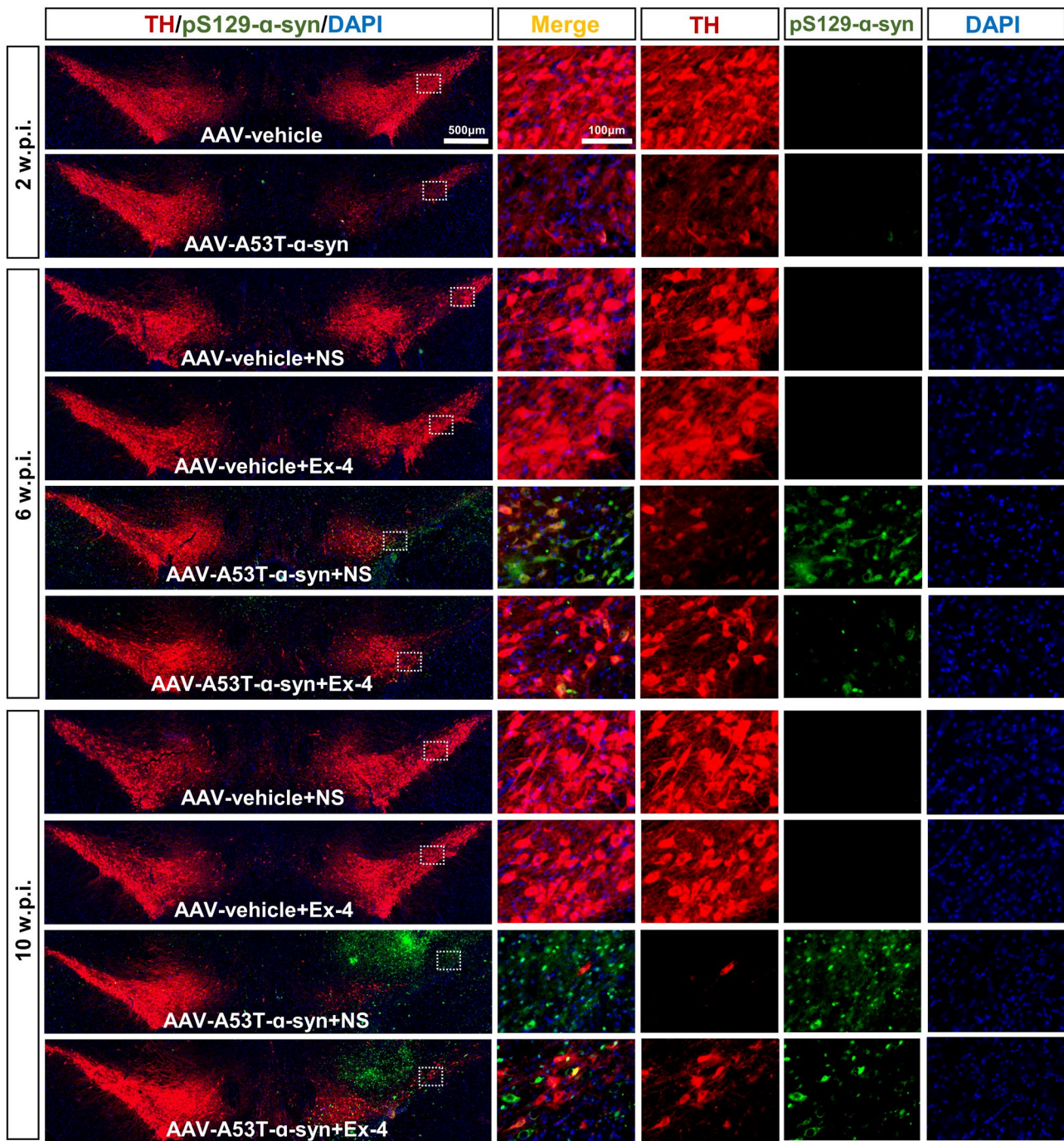


**Fig. 6** AAV-A53T- $\alpha$ -syn-induced PD-like pathology is reduced by Ex-4 treatment. Representative double immunostaining for pSer129- $\alpha$ -syn (green) and TH (red) in the SNpc. The white dashed box in left panel outlines the area of high magnification in the panels shown to the right. The pSer129- $\alpha$ -syn was gradually accumulated in the SNpc region at 2, 6, and 10 w.p.i., accompanied by the increasing degen-

eration of TH-positive neurons, and these pathological changes were largely attenuated by Ex-4 treatment. Similar results were obtained from three biologically independent animals. Ex-4/exendin-4, NS/normal saline, w.p.i. weeks post injection. Scale bars = 500  $\mu$ m and 100  $\mu$ m for low- and high-magnification images

we also added a protein-synthesis inhibitor, CHX, to stop the continuous  $\alpha$ -syn overexpression. We found that  $\alpha$ -syn immunoreactivity was significantly decreased by nearly one-half when solely treated with Ex-4 ( $p = 0.0008$ ; Additional

file 1: Figure S4), which was partially counteracted by 3-MA treatment ( $p = 0.0085$ ). Conversely, the LC3-II/LC3-I ratio of expression was significantly elevated by more than two-fold in the Ex-4 treatment group ( $p = 0.0003$ ; Additional



file 1: Figure S4), which was completely occluded by 3-MA treatment ( $p < 0.0001$ ).

Furthermore, we also investigated the LC3-II/LC3-I expression ratio in AAV-vehicle-injected and AAV-A53T- $\alpha$ -syn-injected rats, which revealed a significantly raised LC3-II/LC3-I ratio in AAV-A53T- $\alpha$ -syn-injected rats under Ex-4 treatment for eight weeks ( $p = 0.0070$ ; Fig. 7d, e). TEM imaging also confirmed activated autophagy in SNpc dopaminergic neurons, as revealed by apparent autophagosome formation after Ex-4 treatment in AAV-vehicle-injected or AAV-A53T- $\alpha$ -syn-injected rats (Fig. 7f).

### Ex-4 Treatment Downregulates the PI3K/Akt/mTOR Pathway

The phosphatidylinositol 3-kinase (PI3K)/protein kinase B (Akt) pathway is an important downstream target of the GLP-1 signaling pathway, which can inhibit autophagy via activation of the mammalian target of rapamycin (mTOR) [4]. To determine the potential mechanism of action of Ex-4, the expression levels of PI3K-p85, p-Akt, and p-mTOR were assessed. Compared with those in the NS control group injected with AAV-vehicle, there was no significant difference in p-Akt or p-mTOR, but they both showed a slight tendency toward overexpression in AAV-A53T- $\alpha$ -syn-injected rats, whereas PI3K-p85 showed a significant upregulation ( $p = 0.0198$ ; Fig. 8 a and b). However, these alterations were completely reversed by Ex-4 treatment, which demonstrated a significant downregulation of the PI3K/Akt/mTOR pathway and resulted in the activation of autophagy.

## Discussion

The major findings of the present study provide preclinical evidence for the neuroprotective effects of Ex-4 by demonstrating that Ex-4 may attenuate TH-positive neuronal loss in the SNpc, alleviate denervation and synaptic dysfunction in the striatum, and ultimately rescue motor deficits in a parkinsonian rat model of  $\alpha$ -synucleinopathy. This model more closely recapitulates the pathophysiology and manifestations of idiopathic PD, allowing for investigation of the accumulation of  $\alpha$ -syn aggregates and the disease-modifying effects of Ex-4 over time. Our findings support the positive effects of Ex-4 on the clearance of pathological pSer129- $\alpha$ -syn and total  $\alpha$ -syn via autophagy, which may be promoted by inhibition of the PI3K/Akt/mTOR signaling pathway.

Classical parkinsonian motor symptoms are recognized as prominent features of PD, which are accompanied by progressive dysfunction within the nigrostriatal dopaminergic pathway. However, minimal motor features representing prodromal PD also indicate remarkable pathological changes in the nigrostriatal system, including

reductions in TH expression and increased accumulation of phosphorylated  $\alpha$ -syn [23]. Additionally, when motor symptoms are present, nearly 30–80% of dopaminergic neurons in the SNpc have already degenerated [24]. In our present study, due to the persistent strong expression of AAV-A53T- $\alpha$ -syn in the SNpc after stereotaxic injection, there was a continuous decline in SNpc dopaminergic neurons starting at 2 w.p.i. After the loss of nearly half of TH-positive SNpc neurons, AAV-A53T- $\alpha$ -syn-injected rats developed apparent motor deficits and asymmetry starting at 6 w.p.i., which was thoroughly rescued by EX-4 treatment at 10 w.p.i. Meanwhile, Ex-4 treatment attenuated TH-positive neuronal loss and nearly stopped any further neuronal loss by the end of the treatment period. VMAT-2 PET/CT is a widely used non-invasive biomarker in clinical practice and diagnosis, which can assess presynaptic dopaminergic terminal deficiency and monitor levels of synaptic dopamine [25, 26]. In our present study, PET/CT scanning revealed a significant decrease in the amount of VMAT-2 at 2 w.p.i. prior to motor dysfunction, indicating an early degeneration in the nigrostriatal dopaminergic system. Additionally, after long-term treatment of Ex-4 since the prodromal phase at 2 w.p.i., the progressive loss of VMAT-2 in the striatum was substantially slowed, although there was still some dopaminergic terminal deficiency at 10 w.p.i. To our knowledge, our present findings are the first to unveil neuroprotective effects of Ex-4 in a progressive parkinsonian rat model, as revealed via PET/CT scanning at different time points. In addition, consistent with protection against VMAT-2 reduction in the striatum (demonstrated by PET/CT scanning), Ex-4 slowed and ultimately halted progressive denervation of SNpc dopaminergic terminals innervating the striatum, as revealed by TH immunostaining. Furthermore, our results of relative striatal fiber density were also comparable with those of VMAT-2 levels measured via PET/CT imaging. Despite discordant clinical and imaging findings in some clinical trials [25], the consistency between VMAT-2-PET/CT scanning and pathological changes in our present study suggests the potential of VMAT-2-PET/CT scanning as a sensitive, objective, and accurate biomarker of neurodegeneration in future clinical trials for evaluating potential neuroprotective treatments. Taken together, our present findings suggest that Ex-4 exerted substantial disease-modifying and symptom-mitigating effects in a rat model and may hold great promise in slowing or even halting the neurodegenerative process in PD. In addition, we also observed mild SUVR reduction in the contralateral striatum despite a unilateral injection of AAV-A53T- $\alpha$ -syn. Although we did not find detectable immunoreactivity of pSer129- $\alpha$ -syn or  $\alpha$ -syn in the left hemisphere (Fig. 6; Additional file 1: Figure S2), we suspect that the bidirectional fiber connections between left

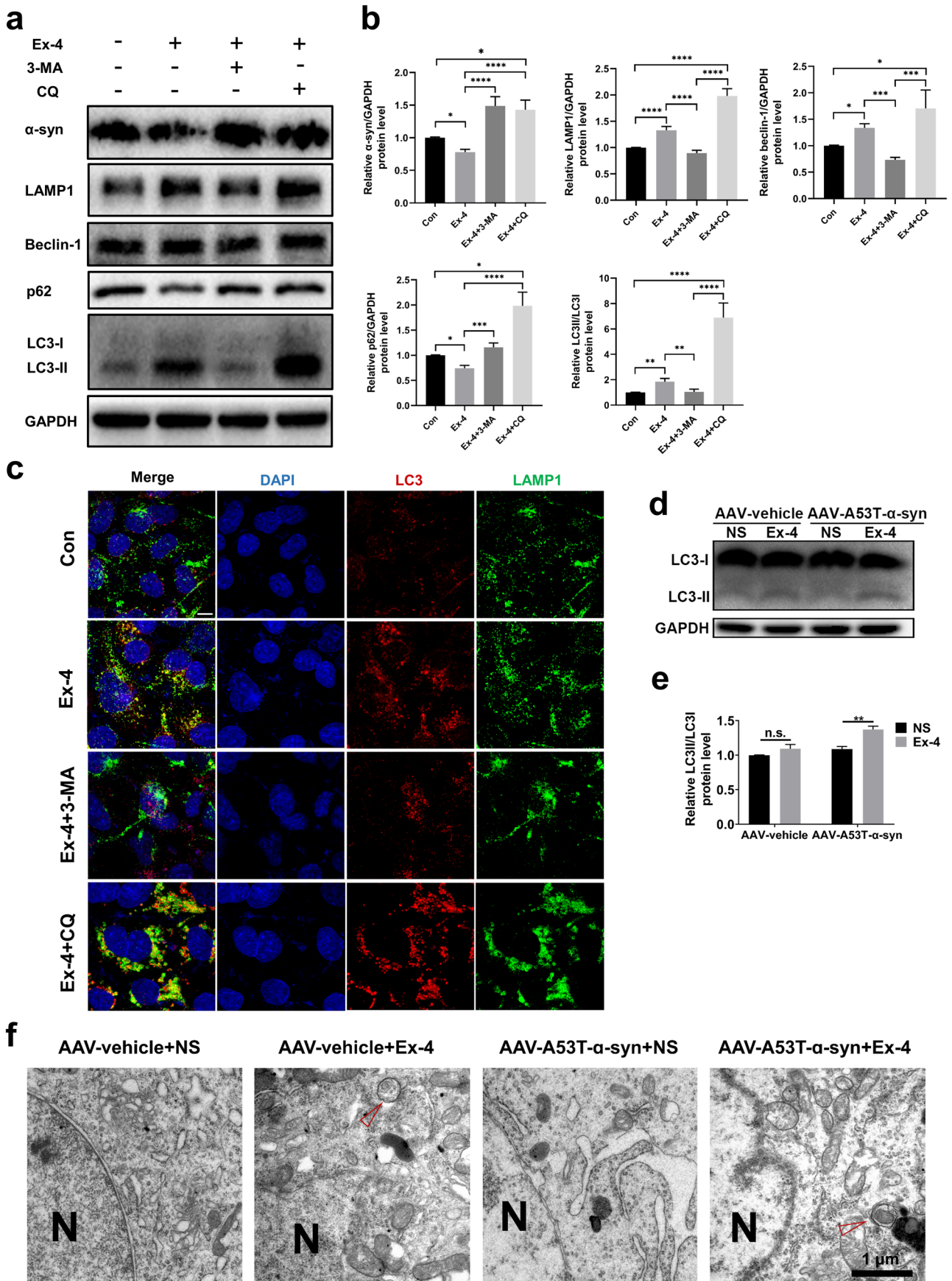




**Fig. 7** Ex-4 treatment enhances autophagy in cell and rat PD models induced by hA53T- $\alpha$ -syn. **(a)** The total lysates of SH-SY5Y cells that overexpressed hA53T- $\alpha$ -syn and were pretreated with PBS (control group), Ex-4 (Ex-4 group), and Ex-4 plus autophagy inhibitor 3-MA (Ex-4+3-MA group) or chloroquine (Ex-4+chloroquine group) were collected for western blotting ( $n = 6$ ). Compared with the control group, the Ex-4 group showed lower  $\alpha$ -syn and p62 levels, accompanied with higher LC3-II/LC3-I ratio and beclin-1 and LAMP1 expression levels, indicating the strong clearance of mutant  $\alpha$ -syn by upregulated autophagic flux, which was completely eliminated by 3-MA and chloroquine treatment. **(b)** Quantification of the western blot in **(a)**. The quantitative analysis was normalized to the GAPDH expression level. Statistical significance was determined using a one-way ANOVA followed by Tukey's post hoc tests. Similar results were obtained from three independent experiments. \* $p < 0.05$ , \*\* $p < 0.01$ , \*\*\* $p < 0.001$ , \*\*\*\* $p < 0.0001$ . **(c)** Representative double immunofluorescence staining with LC3 (red) and LAMP1 (green) antibodies in the SH-SY5Y cells after different treatments ( $n = 4$ ). The LC3B puncta that were positive for LAMP1 were increased in Ex-4 treated SH-SY5Y cells, which was completely eliminated by 3-MA treatment. A mass of LC3- and LAMP1-positive vacuoles was accumulated in chloroquine treated cells, and only few of them were merged. **(d)** The total ventral midbrain lysates of AAV-vehicle-injected and AAV-A53T- $\alpha$ -syn-injected rats with NS or Ex-4 treatment were collected to perform western blotting. Compared with the NS-treated rats, Ex-4-treated rats showed a higher ratio of LC3-II/LC3-I protein level in AAV-A53T- $\alpha$ -syn-injected rats. Each sample was composed of lysates equally pooled from four rats ( $n = 4$ ). **(e)** Quantification of the western blot in **(d)**. Statistical significance was determined using a Two-way ANOVA followed by Tukey's post hoc tests. \*\* $p < 0.01$ ; n.s. not significant. Error bars represent the mean  $\pm$  SEM of at least three independent experiments with similar results. **(f)** Representative TEM images showed that Ex-4 treatment activated autophagosome formation (indicated by red arrowheads) in nigral dopaminergic neurons. Similar results were obtained from three biologically independent animals. Scale bars = 1  $\mu$ m. N nucleus, Ex-4 exendin-4, NS normal saline, 3-MA 3-methyladenine, CQ chloroquine

and right nigrostriatal systems, which integrate them into a structural and functional bilateral entity, may contribute to this phenomenon [27].

Neurotoxic  $\alpha$ -syn is a central component in the pathogenesis of PD, and its etiology is likely multifactorial [28]. The accumulation of  $\alpha$ -syn in vulnerable brain regions induces mitochondrial dysfunction, oxidative stress, and neuroinflammation, and ultimately leads to dopaminergic neuronal death [2]. Misfolded  $\alpha$ -syn gradually becomes insoluble and aggregates within the somata (Lewy bodies) and processes of neurons (Lewy neurites) [29]. In the present study, we employed an  $\alpha$ -syn-overexpression AAV-9 construct to recapitulate the natural disease course of PD and the time-dependent accumulation of  $\alpha$ -syn, which has never been employed in any previous studies that have investigated neuroprotective GLP-1R agonists. Phosphorylation at Ser-129 is the most prevalent (~90%) post-translational modification of  $\alpha$ -syn detected in PD brains containing Lewy bodies [28]. Many studies have shown that hyper-phosphorylation of  $\alpha$ -syn may affect its solubility, membrane-binding properties, and subcellular distribution, thus favoring a pathogenic state [30, 31]. In our

present study, pSer129- $\alpha$ -syn/TH double-immunostaining in AAV-A53T- $\alpha$ -syn-injected rats demonstrated progressive accumulation of pSer129- $\alpha$ -syn within or outside TH-positive neurons over time. Additionally, Ex-4 significantly decreased the amount of pSer129- $\alpha$ -syn co-localized with TH-positive neurons at 6 w.p.i., as well as the total amount of pSer129- $\alpha$ -syn aggregate in the SNpc at 10 w.p.i. In addition, compared with that in AAV-A53T- $\alpha$ -syn-injected rats with NS treatment, more co-localization of pSer129- $\alpha$ -syn in TH-positive neurons was found in the Ex-4 treatment group at 10 w.p.i., which may be attributed to increased survival of dopaminergic neurons in the SNpc. Furthermore, in light of the moderate clearance of total  $\alpha$ -syn (Additional file 1: Figure S2), which may be partially counteracted by persistent expression of AAV-A53T- $\alpha$ -syn, our present findings exhibited stronger clearance of pathogenic pSer129- $\alpha$ -syn induced by Ex-4 treatment. Additionally, Bassil et al. [32] also reported positive effects of Ex-4 on decreasing  $\alpha$ -syn load in the striatum of PLP-SYN mice (overexpressing human  $\alpha$ -syn in oligodendrocytes) that mimicked multiple system atrophy.

Through both in vivo and in vitro experiments, we confirmed the activation of autophagy and clearance of  $\alpha$ -syn induced by Ex-4 treatment. In addition, inhibition of autophagy by 3-MA and chloroquine significantly attenuated degradation of pathogenic  $\alpha$ -syn and reversed the effects of Ex-4. Autophagy is the major intracellular degradation system that eliminates misfolded proteins and produces new building materials and energy for cellular renovation and homeostasis [33]. Furthermore,  $\alpha$ -syn accumulation is linked to alterations in the autophagy-lysosomal pathway and further impairs its function, thus generating a vicious cycle contributing to neuronal death [34]. Previous studies have demonstrated neuroprotective effects of GLP-1R agonists via activating autophagy in an MPTP-induced parkinsonian mouse model [35], SH-SY5Y cell line [36], and a spinal-cord-injury rat model [37]. Additionally, the pleiotropic effects of GLP-1R agonists in the central nervous system have been identified. In some neurotoxin (MPTP, 6-OHDA, rotenone)-based parkinsonian animal and cell models, different GLP-1R agonists have been reported to exert their neuroprotective effects by promoting neurogenesis, neuronal differentiation, and autophagy, as well as by increasing production of trophic factors, impeding neuronal apoptosis, inhibiting microglial activation, and enhancing anti-inflammatory/antioxidant effects [10, 35, 38–41]. Nevertheless, these neurotoxin-based models fail to recapitulate the fundamental pathological events and progressive nature of PD [16], and research on whether Ex-4 can exert neuroprotective effects on  $\alpha$ -syn pathology has been limited. Recently, Yun et al. [11] reported that a long-acting GLP-1R agonist, NLY01 (which is a PEGylated Ex-4), ameliorated dopaminergic dysfunction and parkinsonian behavioral

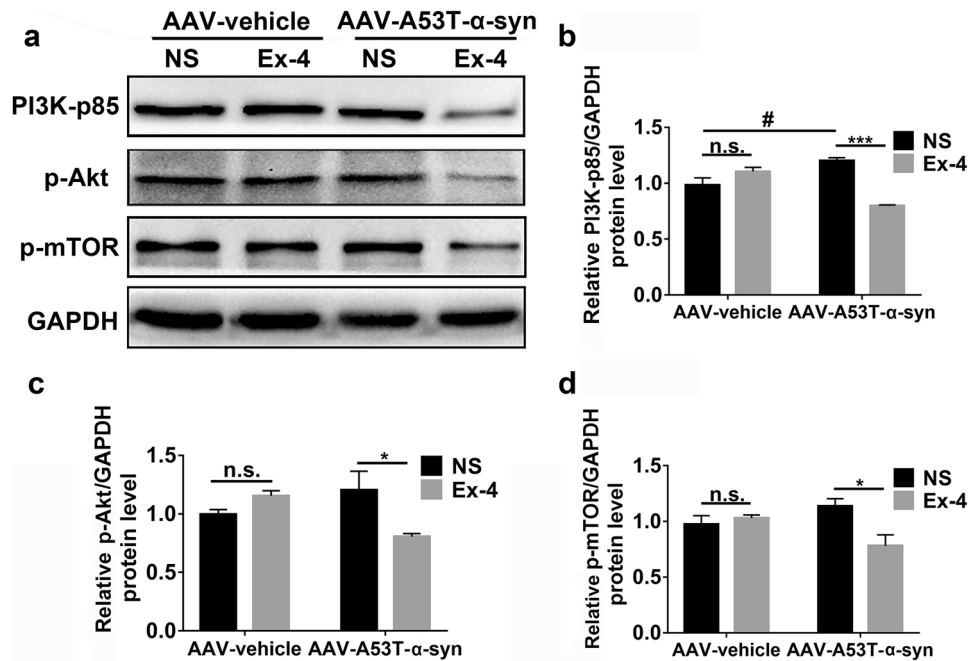


**Fig. 8** Ex-4 treatment attenuates activation of the PI3K/Akt/mTOR signaling pathway in AAV-A53T- $\alpha$ -syn-injected rats. The total ventral midbrain lysates of AAV-vehicle-injected and AAV-A53T- $\alpha$ -syn-injected rats treated with NS or Ex-4 were collected, electrophoresed and immunoblotted. (a) The expression level of PI3K-p85, p-AKT and p-mTOR upon NS or Ex-4 treatment in AAV-vehicle-injected and AAV-A53T- $\alpha$ -syn-injected rats. (b–d) The quantitative analysis of the expression of PI3K-p85, p-AKT, and p-mTOR was normalized to the GAPDH expression level, showing a significant inactivation

of the PI3K/Akt/mTOR pathway in AAV-A53T- $\alpha$ -syn-injected rats with Ex-4 treatment. Error bars represent the mean  $\pm$  SEM of at least three independent experiments with similar results. Each sample was composed of lysates equally pooled from four rats ( $n = 4$ ). Statistical significance was determined using a Two-way ANOVA followed by Tukey's post hoc tests. \* $p < 0.05$ , \*\*\* $p < 0.001$ , NS treatment group versus Ex-4 treatment group; # $p < 0.05$ , AAV-vehicle-injected rats versus AAV-A53T- $\alpha$ -syn-injected rats. n.s. not significant

deficits in an  $\alpha$ -syn-preformed fibril-based PD mouse model and in hA53T  $\alpha$ -syn transgenic mice by blocking microglial activation and the generation of A1 astrocytes. However, Grozdanov et al. [42] revealed that the appearance of pathological  $\alpha$ -syn resulted in robust inflammatory activation of microglia and induced monocyte dysregulation in the periphery, suggesting that there may be more fundamental pathogenesis of  $\alpha$ -syn rather than neuroinflammation in PD. Thus, clearance of pathogenic  $\alpha$ -syn via enhanced autophagy in a parkinsonian rat model of  $\alpha$ -synucleinopathy, revealed by our present findings, may represent a more fundamental mechanism underlying the neuroprotective effects of Ex-4.

The downstream molecular mechanisms of Ex-4 in PD have not been fully elucidated. Evidence from previous studies suggests that insulin resistance contributes to PD via two main pathways: the PI3K/Akt pathway and the mitogen-activated protein kinase (MAPK)/ERK pathway [43, 44]. As an important downstream target of GLP-1R stimulation, the PI3K/Akt pathway plays an important role in regulating normal aging, cellular survival, and autophagy [4]. mTOR is a major regulator of the autophagic process that is modulated by the PI3K/Akt pathway, as well as by starvation, growth factors, and cellular stressors [45]. In

the present study, as enhanced autophagy is indicated by the increased level of LC3-II, an active form of LC3-I, accompanied by the down-regulation of Akt and mTOR, we mainly focused on the PI3K/Akt pathway. We confirmed that Ex-4 treatment reversed abnormal upregulation of the PI3K/Akt pathway in AAV-A53T- $\alpha$ -syn-injected rats with NS treatment and promoted the clearance of pathological  $\alpha$ -syn via enhanced autophagy through inhibition of the PI3K/Akt/mTOR pathway. However, the PI3K/Akt pathway has been revealed to be activated by Ex-4 in some other animal and cell models [36, 46, 47]. Additionally, a secondary analysis of the Exenatide-PD trial also reported elevated activation of the Akt and mTOR signaling pathways in the exosomes of PD patients, which was associated with clinical severity [48]. Taken together, results from experimental models indicate that dysregulation of Akt signaling may be a key component of PD and AD pathogenesis and may influence  $\alpha$ -syn aggregation [49, 50]. In light of these findings, we suspect that loss of regulation of the PI3K/Akt/mTOR signaling pathway may have deleterious effects on neuronal pathophysiological mechanisms, highlighting the importance of maintaining a balance in signaling pathways. In addition, these findings may indicate a regulatory effect

of Ex-4 in maintaining a balance of autophagy and PI3K/Akt signaling.

The present study was unable to show the effects and possible mechanisms of Ex-4 in different forms of  $\alpha$ -syn, such as prefibrillar forms of  $\alpha$ -syn and oligomers, which requires further investigation. And the cell and animal models in this study relied on the high expression of mutant human  $\alpha$ -syn that was not seen in most PD patients, which also requires further confirmation of GLP-1 analogues in other  $\alpha$ -synucleinopathy-based parkinsonian models. Furthermore, in the present study, only female rats were employed. Despite the uncertain effects of gender or hormones in PD [1], further studies involving male animals are needed to confirm the benefit of Ex-4 for clinical use.

Beyond PD, GLP-1R stimulation is protective in models of some other neurodegenerative diseases caused by neurotoxic proteins, such as AD, ALS, and Huntington's disease [8, 9, 51]. In a parkinsonian rat model of  $\alpha$ -synucleinopathy, our present findings provide evidence that neuroprotective benefits of Ex-4 were attributed, at least in part, to the elimination of abnormally aggregated  $\alpha$ -syn via enhanced autophagy, mediated by the regulation of the PI3K/Akt/mTOR pathway. Due to the accumulation of pathogenic misfolded proteins in these neurodegenerative diseases, autophagy contributes to the pathogenesis of these disorders. Because of this, Ex-4 may have broader utility in a variety of neurodegenerative disorders and neurologic injuries involving autophagic dysfunction. Furthermore, in consideration of the disease-modifying effects in preclinical experiments and the positive results in previous clinical trials, GLP-1R agonists hold great promise to be utilized for the development of disease-modifying therapeutic alternatives for PD, which warrants further investigation in PD patients with a delayed-start design or a longer wash-out period in clinical trials.

**Supplementary Information** The online version contains supplementary material available at <https://doi.org/10.1007/s13311-021-01018-5>.

**Acknowledgments** Required Author Forms [Disclosure forms](#) provided by the authors are available with the online version of this article.

**Funding** This work received financial support from the National Natural Science Foundation of China (81771372, 91949118, 81701250, 81801260), Project (2016YFC1306504) from Ministry of Science and technology of China, Shanghai Municipal Science and Technology Major Project (No.2018SHZDZX01, No.2017SHZDZX01) and ZJ Lab, Chinese Medicine Research Project of Shanghai Health and Family Planning Commission (2018JP001), Project of Chinese Academy of Sciences (SKLN-201904), and China postdoctoral science foundation grant (2018T110350).

## Declarations

**Conflict of Interest** The authors declare that they have no conflict of Interest.


## References

- Ascherio A, Schwarzschild MA. The epidemiology of Parkinson's disease: risk factors and prevention. *Lancet Neurol* 2016;15:1257-1272.
- Kalia LV, Lang AE. Parkinson's disease. *Lancet* 2015;386:896-912.
- Lang AE, Espay AJ. Disease Modification in Parkinson's Disease: Current Approaches, Challenges, and Future Considerations. *Mov Disord* 2018;33:660-677.
- Athauda D, Foltynie T. Insulin resistance and Parkinson's disease: A new target for disease modification? *Prog Neurobiol* 2016;145-146:98-120.
- Eng J, Kleinman WA, Singh L, Singh G, Raufman JP. Isolation and characterization of exendin-4, an exendin-3 analogue, from *Heloderma suspectum* venom. Further evidence for an exendin receptor on dispersed acini from guinea pig pancreas. *J Biol Chem* 1992;267:7402-7405.
- Li Y, Perry T, Kindy MS, et al. GLP-1 Receptor Stimulation Preserves Primary Cortical and Dopaminergic Neurons in Cellular and Rodent Models of Stroke and Parkinsonism. *Proc Natl Acad Sci USA* 2009;106:1285-1290.
- Rachmany L, Rachmany L, Tweedie D, et al. Exendin-4 induced glucagon-like peptide-1 receptor activation reverses behavioral impairments of mild traumatic brain injury in mice. *Age* 2013;35:1621-1636.
- Li Y, Duffy KB, Ottinger MA, et al. GLP-1 Receptor Stimulation Reduces Amyloid- $\beta$  Peptide Accumulation and Cytotoxicity in Cellular and Animal Models of Alzheimer's Disease. *J Alzheimers Dis* 2010;19:1205-1219.
- Li Y, Chigurupati S, Holloway HW, et al. Exendin-4 ameliorates motor neuron degeneration in cellular and animal models of amyotrophic lateral sclerosis. *Plos One* 2012;7:e32008.
- Kim S, Moon M, Park S. Exendin-4 protects dopaminergic neurons by inhibition of microglial activation and matrix metalloproteinase-3 expression in an animal model of Parkinson's disease. *J Endocrinol* 2009;202:431-439.
- Yun SP, Kam T, Panicker N, et al. Block of A1 astrocyte conversion by microglia is neuroprotective in models of Parkinson's disease. *Nat Med* 2018;24:931-938.
- Athauda D, Foltynie T. The glucagon-like peptide 1 (GLP) receptor as a therapeutic target in Parkinson's disease: mechanisms of action. *Drug Discov Today* 2016;21:802-818.
- Aviles-Olmos I, Dickson J, Kefalopoulou Z, et al. Exenatide and the treatment of patients with Parkinson's disease. *J Clin Invest* 2013;123:2730-2736.
- Aviles-Olmos I, Dickson J, Kefalopoulou Z, et al. Motor and Cognitive Advantages Persist 12 Months After Exenatide Exposure in Parkinson's Disease. *J Parkinsons Dis* 2014;4:337-344.
- Athauda D, Maclagan K, Skene SS, et al. Exenatide once weekly versus placebo in Parkinson's disease: a randomised, double-blind, placebo-controlled trial. *The Lancet* 2017;390:1664-1675.
- Koprach JB, Kalia LV, Brotchie JM. Animal models of  $\alpha$ -synucleinopathy for Parkinson disease drug development. *Nat Rev Neurol* 2017;18:515-529.
- He Q, Koprach JB, Wang Y, et al. Treatment with Trehalose Prevents Behavioral and Neurochemical Deficits Produced in an AAV alpha-Synuclein Rat Model of Parkinson's Disease. *Mol Neurobiol* 2016;53:2258-2268.
- Koprach JB, Johnston TH, Reyes MG, Sun X, Brotchie JM. Expression of human A53T alpha-synuclein in the rat substantia nigra using a novel AAV1/2 vector produces a rapidly evolving pathology with protein aggregation, dystrophic neurite

- architecture and nigrostriatal degeneration with potential to model the pathology of Parkinson's disease. *Mol Neurodegener* 2010;5:43.
19. Monville C, Torres EM, Dunnett SB. Comparison of incremental and accelerating protocols of the rotarod test for the assessment of motor deficits in the 6-OHDA model. *J Neurosci Methods* 2006;158:219-223.
  20. Liu F, Yang Y, Wu J, et al. Fasudil, a Rho kinase inhibitor, promotes the autophagic degradation of A53T  $\alpha$ -synuclein by activating the JNK 1/Bcl-2/beclin 1 pathway. *Brain Res* 2016;1632:9-18.
  21. Sasaki A, Arawaka S, Sato H, Kato T. Sensitive western blotting for detection of endogenous Ser129-phosphorylated  $\alpha$ -synuclein in intracellular and extracellular spaces. *Sci Rep* 2015;5.
  22. Levine B, Kroemer G. Autophagy in the Pathogenesis of Disease. *Cell* 2008;132:27-42.
  23. Chu Y, Buchman AS, Olanow CW, Kordower JH. Do subjects with minimal motor features have prodromal Parkinson disease? *Ann Neurol* 2018;83:562-574.
  24. Cheng HC, Ulane CM, Burke RE. Clinical progression in Parkinson disease and the neurobiology of axons. *Ann Neurol* 2010;67:715-725.
  25. Brooks DJ, Pavese N. Imaging biomarkers in Parkinson's disease. *Prog Neurobiol* 2011;95:614-628.
  26. de la Fuente-Fernandez R, Lu JQ, Sossi V, et al. Biochemical variations in the synaptic level of dopamine precede motor fluctuations in Parkinson's disease: PET evidence of increased dopamine turnover. *Ann Neurol* 2001;49:298-303.
  27. Henrich MT, Geibl FF, Lee B, et al. A53T- $\alpha$ -synuclein overexpression in murine locus coeruleus induces Parkinson's disease-like pathology in neurons and glia. *Acta Neuropathol Commun* 2018;6:39.
  28. Rocha EM, De Miranda B, Sanders LH. Alpha-synuclein: Pathology, mitochondrial dysfunction and neuroinflammation in Parkinson's disease. *Neurobiol Dis* 2018;109:249-257.
  29. Goedert M, Spillantini MG, Del TK, Braak H. 100 years of Lewy pathology. *Nat Rev Neurol* 2013;9:13-24.
  30. Zhou J, Broe M, Huang Y, et al. Changes in the solubility and phosphorylation of  $\alpha$ -synuclein over the course of Parkinson's disease. *Acta Neuropathol* 2011;121:695-704.
  31. Visanji NP, Wislet-Gendebien S, Oschipok LW, et al. Effect of Ser-129 Phosphorylation on Interaction of  $\alpha$ -Synuclein with Synaptic and Cellular Membranes. *J Biol Chem* 2011;286:35863-35873.
  32. Bassil F, Canron M, Vital A, et al. Insulin resistance and exendin-4 treatment for multiple system atrophy. *Brain* 2017;140:1420-1436.
  33. Mizushima N, Komatsu M. Autophagy: renovation of cells and tissues. *Cell* 2011;147:728-741.
  34. Xilouri M, Brekk OR, Stefanis L. Autophagy and Alpha-Synuclein: Relevance to Parkinson's Disease and Related Synucleopathies. *Mov Disord* 2016;31:178-192.
  35. Zhang L, Zhang L, Li L, Hölscher C. Neuroprotective effects of the novel GLP-1 long acting analogue semaglutide in the MPTP Parkinson's disease mouse model. *Neuropeptides* 2018;71:70-80.
  36. Panagaki T, Michael M, Hölscher C. Liraglutide restores chronic ER stress, autophagy impairments and apoptotic signalling in SH-SY5Y cells. *Sci Rep* 2017;7.
  37. Li H, Zhao X, Zhang X, et al. Exendin-4 Enhances Motor Function Recovery via Promotion of Autophagy and Inhibition of Neuronal Apoptosis After Spinal Cord Injury in Rats. *Mol Neurobiol* 2016;53:4073-4082.
  38. Bertilsson G, Patrone C, Zachrisson O, et al. Peptide hormone exendin-4 stimulates subventricular zone neurogenesis in the adult rodent brain and induces recovery in an animal model of parkinson's disease. *J Neurosci Res* 2008;86:326-338.
  39. Abdelsalam RM, Safar MM. Neuroprotective effects of vildagliptin in rat rotenone Parkinson's disease model: role of RAGE-NF $\kappa$ B and Nrf2-antioxidant signaling pathways. *J Neurochem* 2015;133:700-707.
  40. Yuan Z, Li D, Feng P, et al. A novel GLP-1/GIP dual agonist is more effective than liraglutide in reducing inflammation and enhancing GDNF release in the MPTP mouse model of Parkinson's disease. *Eur J Pharmacol* 2017;812:82-90.
  41. Luciani P, Deledda C, Benvenuti S, et al. Differentiating effects of the glucagon-like peptide-1 analogue exendin-4 in a human neuronal cell model. *Cell Mol Life Sci* 2010;67:3711-3723.
  42. Grozdanov V, Bousset L, Hoffmeister M, et al. Increased Immune Activation by Pathologic alpha-Synuclein in Parkinson's Disease. *Ann Neurol* 2019;86:593-606.
  43. Aviles-Olmos I, Limousin P, Lees A, Foltynie T. Parkinson's disease, insulin resistance and novel agents of neuroprotection. *Brain* 2013;136:374-384.
  44. Kleindridders A, Cai W, Cappellucci L, et al. Insulin resistance in brain alters dopamine turnover and causes behavioral disorders. *Proc Natl Acad Sci* 2015;112:3463-3468.
  45. Heras-Sandoval D, Pérez-Rojas JM, Hernández-Damián J, Pedraza-Chaverri J. The role of PI3K/AKT/mTOR pathway in the modulation of autophagy and the clearance of protein aggregates in neurodegeneration. *Cell Signal* 2014;26:2694-2701.
  46. Ji C, Xue G, Lijun C, et al. A novel dual GLP-1 and GIP receptor agonist is neuroprotective in the MPTP mouse model of Parkinson's disease by increasing expression of BDNF. *Brain Research* 2016;1634:1-11.
  47. Xie Z, Enkhjargal B, Wu L, et al. Exendin-4 attenuates neuronal death via GLP-1R/PI3K/Akt pathway in early brain injury after subarachnoid hemorrhage in rats. *Neuropharmacology* 2018;128:142-151.
  48. Athauda D, Gulyani S, Karnati HK, et al. Utility of Neuronal-Derived Exosomes to Examine Molecular Mechanisms That Affect Motor Function in Patients With Parkinson Disease. *JAMA Neurol* 2019;76:420.
  49. Kim SR, Ries V, Cheng H, et al. Age and  $\alpha$ -synuclein expression interact to reveal a dependence of dopaminergic axons on endogenous Akt/PKB signaling. *Neurobiol Dis* 2011;44:215-222.
  50. Griffin RJ, Moloney A, Kelliher M, et al. Activation of Akt/PKB, increased phosphorylation of Akt substrates and loss and altered distribution of Akt and PTEN are features of Alzheimer's disease pathology. *J Neurochem* 2005;93:105-117.
  51. Sayed NH, Fathy N, Kortam MA, Rabie MA, Mohamed AF, Kamel AS. Vildagliptin Attenuates Huntington's Disease through Activation of GLP-1 Receptor/PI3K/Akt/BDNF Pathway in 3-Nitropropionic Acid Rat Model. *Neurotherapeutics* 2020;17:252-268.



## Authors and Affiliations

Lu-Lu Bu<sup>1</sup> · Yi-Qi Liu<sup>1</sup> · Yan Shen<sup>1</sup> · Yun Fan<sup>1</sup> · Wen-Bo Yu<sup>1</sup> · Dong-Lang Jiang<sup>2</sup> · Yi-Lin Tang<sup>1</sup> · Yu-Jie Yang<sup>1</sup> · Ping Wu<sup>2</sup> · Chuan-Tao Zuo<sup>2</sup> · James B. Koprach<sup>1,3</sup> · Feng-Tao Liu<sup>1</sup> · Jian-Jun Wu<sup>1</sup> · Jian Wang<sup>1</sup> 

✉ Jian Wang  
wangjian\_hs@fudan.edu.cn

Feng-Tao Liu  
liufengtao@fudan.edu.cn

Jian-Jun Wu  
wujianjun@fudan.edu.cn

<sup>1</sup> Department of Neurology & National Clinical Research Center for Aging and Medicine, Huashan Hospital, Fudan University, Shanghai 200040, China

<sup>2</sup> PET Center, Huashan Hospital, Fudan University, Shanghai 200235, China

<sup>3</sup> Krembil Research Institute, Toronto Western Hospital, University Health Network, Toronto, ON M5T 2S8, Canada